European Commission

# JRC TECHNICAL REPORTS

Project: EURAD

WP8: Spent fuel characterisation and evolution until disposal (SFC)

Task 3: Behaviour of nuclear fuel and cladding after discharge

Sub-task 3.1: Thermo-mechanical-chemical properties of the SNF rods and cladding

Document: Progress report, part-A

Period: June 2019 – September 2020

# PART-A: Mechanical properties of spent nuclear fuel rods

**Sensitive**
2020

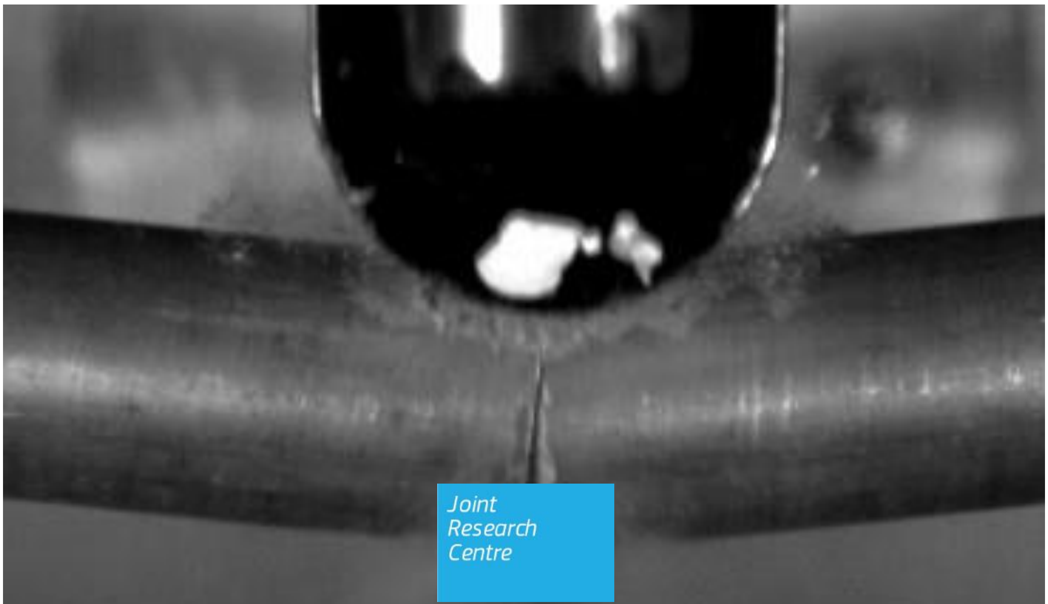

**Contact information**
Name: D. Papaioannou
Address: JRC-KARLSRUHE, UNIT G.III.8 Waste Management, P. O. BOX 2340, D-76125 Karlsruhe/Germany
Email: Dimitrios.Papaioannou@ec.europa.eu
Tel.: +49 7247 951-557

**EU Science Hub**
https://ec.europa.eu/jrc

JRC122564

Karlsruhe: European Commission, 2020



How to cite this report: Papaioannou, D., Nasyrow, R., Gretter, R., Fongaro, L. and Rondinella, V., *PART-A: Mechanical properties of spent nuclear fuel rods*, European Commission, Karlsruhe, 2020, JRC122564.

# Contents

## Acknowledgments

The authors of this report and scientists in duty of the EURAD project at JRC-KARLSRUHE are grateful to Dr. E. Schweitzer, Dr. K. Münchow and Dr. P. B. Hoffmann from Framatome GmbH and Dr. S. Caruso from Goesgen NPP for their kind support in this research programme. We are particularly grateful for making available the MOX spent nuclear fuel rod employed for the mechanical tests.

## Authors:

D. Papaioannou (Interpretation and reporting)

R. Nasyrow (Mechanical testing)

R. Gretter (Sample preparation)

L. Fongaro (IA, H-measurements)

V. Rondinella (Reporting, reviewing)

## Progress summary

This report describes activities carried out at JRC-KARLSRUHE in the frame of the EURAD project, WP8, Task 3, Subtask 3.1 in the period between June 2019 and August 2020. Progress was made in the following areas:

- Maintenance and completion of the hot cells setup required for the mechanical tests on SNF rod segments and specimens;
- A gravitational impact test on a SNF rod segment;
- A ring compression test on an irradiated cladding specimen.

## Abstract

During reactor operation, the mechanical properties of a spent nuclear fuel (SNF) rod are significantly altered by the radiation damage and thermomechanical effects associated with the irradiation conditions in the reactor core. After discharge, the accumulation of alpha-decay radiation damage and other processes associated to potential thermal variations occurring during interim storage, contribute to further ageing of the nuclear fuel rod. However, during all stages of the SNF management (handling, transportation, storage, retrieval, packaging and transportation to final disposal site, if not reprocessed) safety must be guaranteed. The mechanical stability of spent nuclear fuel rods against normal or accidental external stresses is therefore of key importance. In particular, as the necessity of extended interim storage periods is nowadays considered, retaining good mechanical properties after long storage periods is of high relevance.

In the frame of the project EURAD, WP8, Task 3, Sub-task 3.1, specific tests aiming to assess the response of spent fuel rods to mechanical loads are conducted in the hot cell facilities at JRC–KARLSRUHE. Representative reference experimental data obtained from own developed devices are collected in the laboratory: 3-point bending and impact tests on sealed pressurised segments of SNF rods and ring compression tests (RCT) on irradiated cladding materials are performed.

During the reporting period, a gravitational impact test on a spent fuel rod segment at the upper end of the fuel stack was performed. In parallel, the spectrum of testing capabilities in hot cell has been further enriched with a new setup to carry out RCT on irradiated claddings. The first test on a cladding ring obtained from a SNF rod has been successfully completed.

# 1 Introduction

In many countries producing nuclear energy, the interim storage of spent nuclear fuel (SNF) may be extended up to 100 years and beyond, until the geologic repositories for final disposal will be constructed and commissioned [1]. At the end of the storage, the temporarily stored fuel rods must be retrieved, handled, repacked and transported to their ultimate disposal facilities. In this perspective, it is important to address the mechanical integrity of used fuel rods during and after storage, under normal operational or even accidental conditions. In extreme cases of a transport accident for instance, SNF rods might be fractured and fuel may be released and disperse in the cask. The fuel release must not generate radiological consequences exceeding the safety limit; even in the worst case of reconfiguration and accumulation inside the transport container, the criticality safety must be ensured.

The mechanical properties of nuclear fuel rods change significantly during their operational life in the reactor. Irradiation of the fuel induces gas production and accumulation of fission products in the fuel, restructuring phenomena (e.g. the development of high burn-up structure (HBS) at the fuel periphery [2]), cracking and swelling, gap closing and formation of pellet-cladding interaction (PCI) layer, which consequently enhances the hoop stress on the cladding. Presence of deleterious compounds in the PCI can also chemically affect the reliability of the cladding, whose ductility is disturbed by irradiation and hydrogenation. Despite the lower dose rates and temperatures during storage than during irradiation, the fuel alterations do not end with discharge from the reactor. The continuous alpha-decay and helium build-up, in particular after extended storage periods, may result in further damage in the fuel and indirectly, in the cladding [3], [4]. In addition, heating and cooling processes occurring during handling (discharge, followed by wet-dry interim storage) may affect the configuration of hydrogen in the cladding, causing hydride reorientation phenomena, which in turn affects cladding ductility and mechanical stability. All these modifications may affect the response of spent fuel rods to external mechanical solicitations that might occur during normal or accidental conditions.

Several attempts, mostly modelling approaches and rather limited experimental studies, have been conducted by the international research community to enrich the knowledge of the underpinning mechanisms affecting the mechanical properties of SNF rods. The majority of the experimental works are focussed on irradiated cladding properties by performing tests on defueled cladding ring specimens (ring compression tests). However, results from experiments on the composite fuel-cladding configuration, i.e. real SNF rods are extremely rare. Direct tests on irradiated fuel rods require technologically complicated facilities and apparatus (hot cells, specific equipment operated via remote control, etc.); moreover, they involve using relatively large-size highly radioactive samples, producing correspondingly large amounts of spent fuel waste; therefore, they are quite expensive and technically difficult to perform.

A relevant work has been performed by Dallongeville et al. during a joint project, the Fuel Integrity Project, between BNFL Nuclear Sciences and Technology Services and Cogema Logistics (Areva Group) [5]. In this work bending tests carried out on fresh and SNF rods with average burn-up of 50 GWd/tHM. The project objective was to assess the response of Light Water Reactor (LWR) fuel assemblies (FA) during 9 meters regulatory test drops. The bending test span corresponded roughly to the fuel pin inter-grid distance. Fuel rod failures were observed at about 35mm net lateral deflection. Ring compression tests or as called by the authors, hull lateral compaction tests were also performed.

At the JRC-KARLSRUHE, already in 2008, a simple free-falling hammer device inducing fuel rupture events was developed and installed in a hot cell. The impact tests were performed on irradiated commercial LWR $UO_2$ fuel segments with burn-ups between ~19 and ~74 GWd/tHM. The studies were carried out in the frame of collaboration and with the support of GNS (Germany) and AREVA NP and generated important out-comes. Although the rigidly fixed SNF rod specimens ruptured over 3 breakages, totally 3.9 to 5.6 g of coarse fuel fragments were released, i.e. 1.3 g to 1.9 g of fuel per breakage. Details of those pilot tests can be found in [3], [6] and [7].

In 2016, a new experimental campaign was initiated at JRC-KARLSRUHE to establish a basis of reference data and provide reliable conclusions by performing tests on SNF rod segments with own developed dedicated equipment. The new campaign is partly based on collaborations with Framatome GmbH (Germany), NAGRA (Switzerland), NPP Goesgen (Switzerland) and BAM (Germany) [8], [9] and aims to determine the fuel rod response to external loads up to rod failure. Segments with different properties (burn-up, fuel composition, history, cladding, etc.) are pressurized to the original rod pressure and subjected to quasi static – bending – or dynamic – impact – mechanical loading experiments. The critical fracture load (or, better, energy) and the fuel mass released are determined. Thorough characterisation of the fuel rod and of the resulting specimens is carried out before and after each experiment for a comprehensive evaluation of the SNF rods behaviour.

The studies proposed by JRC-KARLSRUHE for the EURAD project will extend the reference basis of data with results covering additional burn-ups of $UO_2$ SNF rods, and extend the knowledge with experiment on a MOX SNF rod. The characterization of mass release during fracturing tests will include distribution size analysis of the fuel particles released, cladding metallography at fracture point to investigate hydride population and orientation and local hydrogen content measurement with the hot-gas extraction technique. The proposal also includes ring compression tests on defueled cladding rings. These experiments will be exclusively performed to support with experimental data the modelling works performed at BAM and UPM on the irradiated cladding properties.

# 2 Experimental set up

The experiments are conducted in the hot-cell facilities at JRC–KARLSRUHE with basically two in-house developed devices, comprehensively described in [10] [11] [12] [13] for 3-point bending and gravitational impact tests on fuelled, pressurised SNF rod segments. During the reporting period, for the programme needs within the EURAD project, the bending device has been equipped with new components to perform RCT of irradiated cladding specimens. Load-deflection curves are generated in the 3-point bending and RCT, whereas a high-speed camera records the rod rupture during impact tests.

The force/energy required for a fuel rod to fail is determined under the experimental boundary conditions. As the accidental scenario conditions that could be tested are very numerous, it has been decided to study the SNF mechanical integrity under two reference conditions by applying quasi-static or dynamic loads. The acquired data are correlated to properties and processes that potentially affect the SNF mechanical stability. In addition to post irradiation examinations performed on the fuel rod at previous times, including many non-destructive or destructive hot cell techniques, fuel and cladding of the tested specimens are thoroughly examined after the mechanical testing. Metallography at the direct vicinity of the failure location to investigate the hydride morphologies, population and orientation is implemented, whilst the local Hydrogen content is determined by means of the hot-gas extraction method. After each impact test, the released fuel particles are collected and examined by scanning electron microscopy (SEM) for morphology and size distribution analysis.

## 2.1 Bending device

The 3-point bending device is schematically shown in **Figure 1**. The apparatus consists of a force transmitter fixed on a loading column, which is driven by a step-motor perpendicular to the sample axis at constant preselected (slow) speed between 4 and 17 μm/s. The force transmitter, the "deflector", has a concave round contact surface (partly seen in **Figure 1**(b)), adjusted to the cladding shape, so that no other side or edge load is applied on the fuel rod segment during experiment.

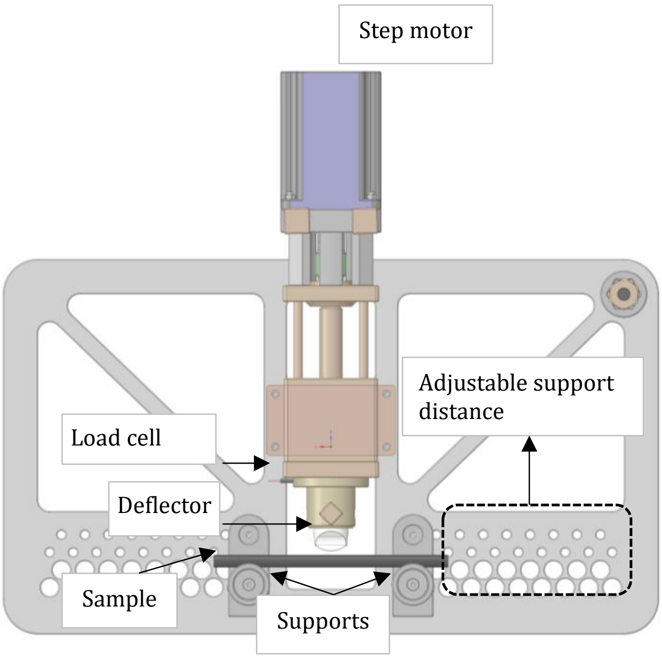


(a)

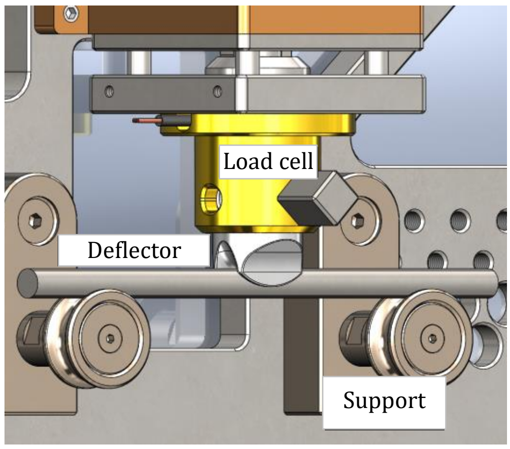


(b)

**Figure 1.** Overview of the bending device (a) and zoom in of the specimen positioning and deflector (b).

The flexible modular design of the device allows using different loading transmitters, and, thanks to removable supports, different specimen lengths. The geometrical configuration of the device follows the prerequisites of a standard bending test as specified in the ISO 7438 standard [14]. The device is equipped with sensors for simultaneous acquisition of the applied load and the sample's deflection and internal pressure of the segment (described in section 2.4).

## 2.2 Conversion to RCT device

By exchanging some parts in the above-described bending device, the equipment is capable to carry out RCT on cladding ring specimens. At the lower side of the machine's metallic frame, a horizontal table can be fixed, where the cladding specimen is placed and kept in position by means of side holders until it comes in touch and starts to be stressed by the flat cylindrical deflector.

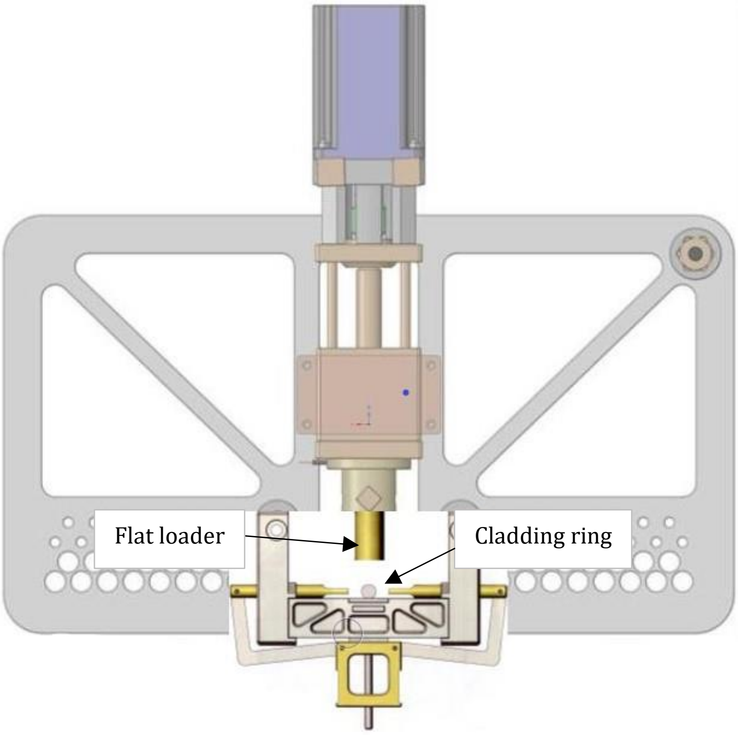


**Figure 2.** Overview of the modified bending device to perform ring compression tests (RCT) on irradiated cladding materials.

## 2.3 Gravitational impacting device

The apparatus for impact tests is based on the same principles as the older one used to perform the experiments reported in [6] and schematically shown in **Figure 3**. The impacting occurs in a closed chamber, where the released material (basically fuel, but also pieces of the cladding and the outer cladding oxide layer) is completely captured. The coarse fragments are collected at the bottom thanks to the funnel shape of the down chamber interior shown in **Figure 4**, whereas the fine aerosol particles settle on the internal walls, or are captured on the particulate filter of an integrated aspiration system (visible in **Figure 4**). The impact of the specimen is recorded by a high-speed digital camera (2000 frames/s) placed on the window of the chamber, which is strongly illuminated by a series of LEDs positioned inside. The specimen is impacted by the "impactor", a body (hammer) falling through a vertical guiding column.

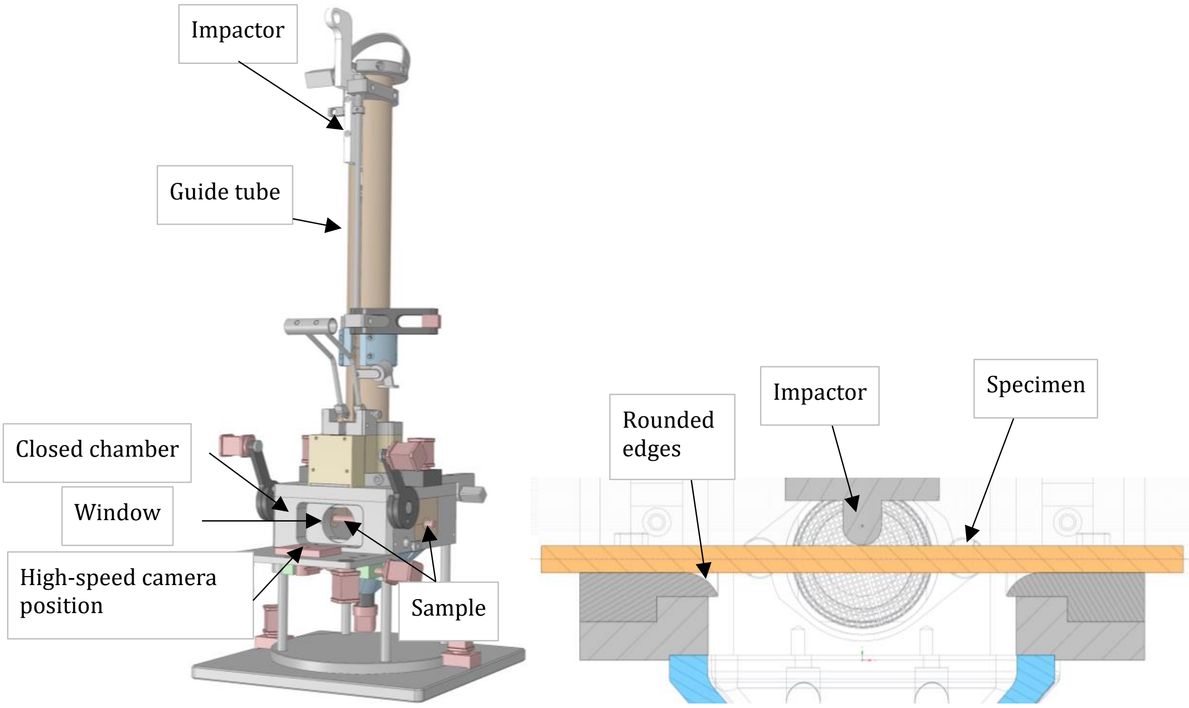


(a) (b)

**Figure 3.** Overview of the impacting device (a) and zoom in of the specimen positioning and impactor (b).

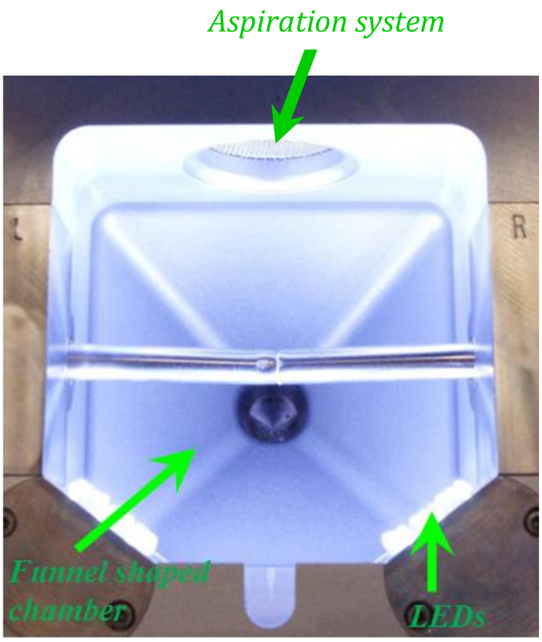


**Figure 4.** Inside view of the closed test space of the impact device after a dummy cold test (Zr-alloy tube filled with alumina pellets). Bigger fragments are collected at the bottom, whereas the smaller and aerosol particles are deposited on the chamber walls.

As far as possible the designs of the bending and impact devices have been kept mutually consistent. In both experiments, the specimens are bent or impacted by rounded compactors, as shown in **Figure 1**(b) and **Figure 3** (b). The main difference is related to the velocity of the impactor and bending deflector in the two experiments, enabling direct comparison of the results in both configurations. Indeed, the velocity of the falling hammer at point of impact is 3.5 m/s, i.e. at least $2x10^6$ times faster than in the 3-point bending test.

## 2.4 Sample assembling for impacting and bending

The cut segments were pressurized at their original pressures, as it had been measured at the time of the PIE and hermetically sealed with proper tube fittings. A typical specimen for mechanical testing is shown in the photograph of **Figure 5**. Using exact tube fittings to preserve the required tightness, 25-27 cm long segments cut from SNF rods are connected to a Helium gas flask, pressurised to the desired pressure and disconnected, after closing the attached gas valve. A pressure transducer, fixed on the other end of the segment provides continuous pressure control and instant detection of the rupture/crack, which is very important for the bending tests.

**Figure 5**. Gas tight specimen assembly connected to pressure gauge and with attached pressure transducer, ready for mechanical testing.

# 3 Tests and results

## 3.1 Samples

During the reporting period, one RCT and one impact test were carried out. The sample for the RCT has been cut from the upper plenum of a PWR SNF rod with average burn-up (BU) 67 GWd/tHM. The cut ring, labelled as T16-9-3, 10 mm in length, originates only 6.5 mm above the first pellet of the fuel stack; therefore, no defueling was necessary. Based on previous experience, the plenum cladding at the direct vicinity of the fuel stack might contain hydrides. Dedicated measurements with the hot extraction method as well as metallographic observation are foreseen and will be performed within the next reporting period, to gain detailed information about the overall hydrogen content and the hydrides morphology of the material tested. It is expected that at the original location of the sample tested, the total hydrogen content will be lower than 300 ppm measured at a central position of the same SNF rod and shown in [15] (FIG. 10b and FIG. 11b), [16] (slide no. 18), [17] (slide no. 17). The cladding is a duplex with outer liner and its composition is listed in [15] (TABLE 1).

The specimen for the impact test originates from a PWR SNF rod with heterogeneous MOX fuel irradiated up to BU 60.6 GWd/tHM. It has been taken from the middle rod axis, i.e. from the high BU zone. It has been pressurized at slightly over 50 bar and sealed as shown in **Figure 5**. After carrying out the 3-point bending test on the same SNF segment, post-test examinations including hydrogen content measurements and metallography analysis were planned, too, as for the RCT sample. During previous post irradiation examinations (PIE) of the same SNF rod, measurements at neighbour locations of the specimen studied indicated <250 ppm total hydrogen content in the cladding.

## 3.2 RCT on the cladding sample T16-9-3

In the RCT, the applied load and corresponding displacement were continuously recorded. The loading proceeded with low speed, 4.9 µm/s translation of the loading system. During the experiment, a video has been recorded with a camera installed outside the hot cell. The obtained data are plotted in **Figure 6**, together with the curve of a cold test on a fresh, non-irradiated Zr-4 cladding ring of the same dimensions, for comparison reasons. The attached photographs are illustrating the sample deformation at characteristic instants during experiment and were placed (middle of the photograph) at the corresponding displacements.

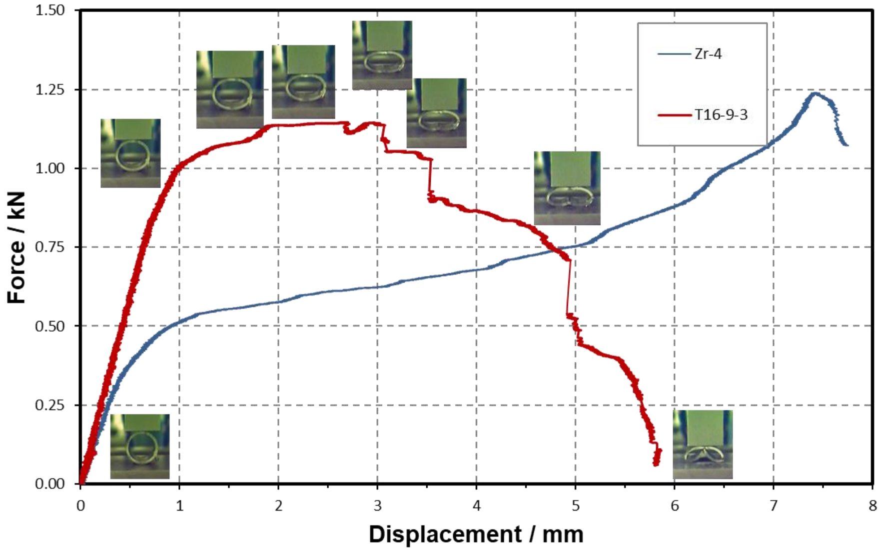


**Figure 6**. Load versus displacement in the RCT on the duplex cladding sample T-16-9-3. The photographs illustrate the sample deformation at relevant times/displacements during the experiment.

Despite the fact that the 2 samples described on the plot presented differences in metal composition and structure (duplex/liner vs. homogeneous Zr-4), significant effects due to irradiation can be observed by comparing the two plotted curves. Although the highest load applied is quite similar (~1.14 and 1.25 kN, respectively), the overall displacement of the irradiated sample till its complete cracking in 4 pieces is much shorter. The cracking took place progressively; four well-distinguishable load drop steps are observed at ca. 2.6, 3.1, 3.5 and 4.9 mm displacement. In both cases the elastic range extends up to ~ 1 mm displacement, but with double load for the irradiated sample (1 vs. 0.5 kN).

### 3.3 Impact test on the MOX SNF rod segment

A video recorded with the high-speed camera of the device chamber has documented the experiment. The video will be submitted separately to his report and will be used to calculate the transmitted energy from the hammer to the specimen, which caused the rupturing by Image Analysis (IA). As shown in [17] (slide no. 18), by means of the high-speed camera video, the transmitted energy from the hammer to the specimen can be calculated based on the falling velocity change between the first contact moment and the final rupturing.

Four representative photographs taken during the impact are presented in **Figure 7**. Upon the first contact of the hammer, the outer oxide layer shatters; thereafter follow the cracking, depressurization and major fuel release from the fractured rodlet.

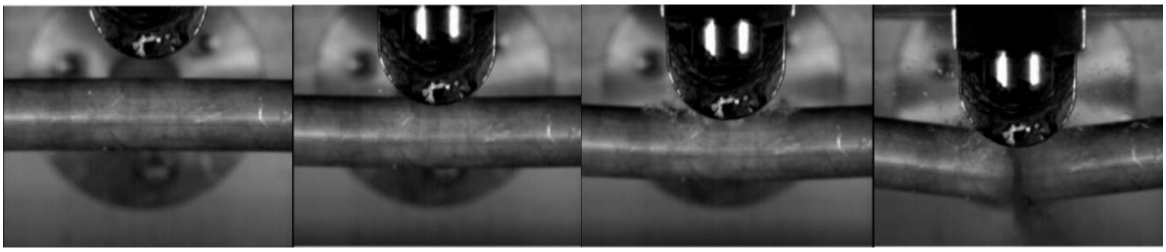

**Figure 7.** Photograph sequence during impacting of the MOX specimen.

To determine the amount of fuel released during the impact, the fuel rodlet and the fractured segments are weighed before and after the test. The mass difference after the fracture corresponds to the total amount of fuel released. Thus, it has been measured that **totally 2.24 g were released** upon fracturing the spent fuel segment. Since the impact takes place in a closed chamber connected to an aspiration system through a particulate filter, the released fuel particles are contained within the testing setup. Upon fracturing the fuel rod segment, the heavy fragments fall in a vessel at the bottom of the chamber. The fine particles deposit onto the walls and surfaces in the testing chamber or are collected onto the micro-filters of the aspiration system.

The heavy fragments collected at the bottom of the testing chamber after the experiment were sieved and weighed to sort them according to their size. The result of the characterization of the heavy fuel particles is listed in **Table 1**.

**Table 1**. Sizes and masses of the fragments collected at the bottom of the chamber

| **Size (ECD) [µm]** | **Mass [g]** |
|---|---|
| 0-90 | 0.12 |
| 90-250 | 0.29 |
| 250-630 | 0.50 |
| 630-1000 | 0.43 |
| >1000 | 0.70 |
| **Total** | **2.04** |

The "missing" 0.2 g (0.9 % of the total mass released) consisted of aerosol and fine particulate deposited on the inner walls of the testing chamber or collected on the filters coupled with the aspiration pump which "vacuumed" the test chamber before, during and after the impact. The collected fine particles will be submitted to scanning electron microscopy (SEM-EDS) and characterized in terms of size distribution. As a complement to the micro-filters, swipes of the testing chamber walls were made at different locations to collect fine particles deposited on the walls. Both filters and swipes will be examined.

**The main conclusion of this first impact test on a MOX SNF rod segment at this stage of the analysis is that the released mass upon fracturing is limited, only 2.24 g. This amount is much less than the mass of a single fuel pellet; furthermore, it is in the same range, comparable to the release from a $UO_2$ SNF rod with similar BU. The fuel mass released in several tests, including the present test on MOX fuel, is plotted as a function of fuel burnup in Fig. 8.**

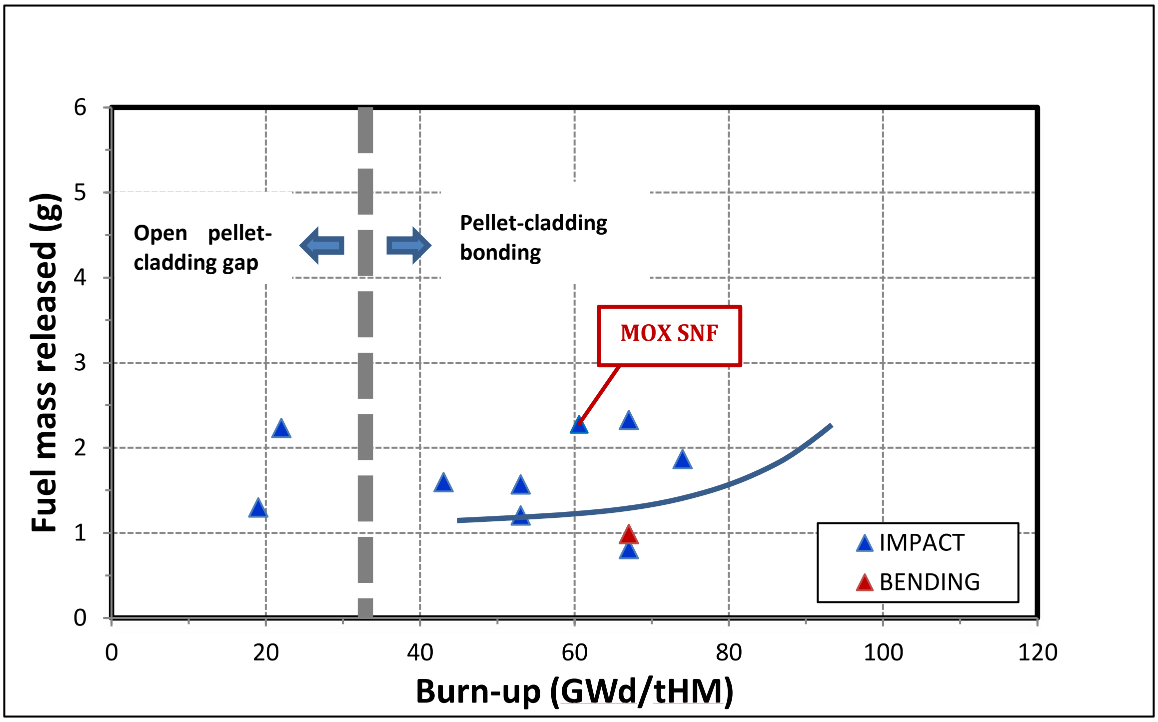


**Figure 8.** Fuel mass released during impact and bending tests as a function of fuel burnup. The impact test result of a MOX SNF rod is in fair compliance with data obtained in tests of $UO_2$ SNF rod segments ( [17], slide no. 22).

# 4 Next tasks

The continuation of the studies during the next reporting period, i.e. till September 2021 contains:

- Hydrogen measurements and metallography related to the above reported RCT and impact tests;
- SEM/EDS on the fine particles collected after the above reported impact test;
- Image Analysis (IA) of the high-speed camera video of the above reported impact test;
- 3-point bending test on the MOX SNF rod on the same segment as the above reported impact test;
- Calibration of the sensors (force and displacement) of the bending device; system alteration with new components;
- RCT on 1 or 2 irradiated cladding samples.

## References


[1] "Extended Storage Collaboration Program International Subcommittee Report," EPRI Report 1026481, 2012.

[2] V. V. Rondinella and T. Wiss, "The high burnup structure in nuclear fuel," *Materials Today,* vol. 13, pp. 24-32, 2010.

[3] V. V. Rondinella, T. Wiss, D. Papaioannou, R. Nasyrow, F. Cappia, S. Van Winckel, D. Serrano-Purroy and D. Wegen, in *Proc. International High-Level Radioactive Waste Management Conference (IHLRWM)*, Charleston, U.S.A., 2015.

[4] T. Wiss et al., *J. Nucl. Mater.,* vol. 451, pp. 198-206, 2014.

[5] M. Dallongeville, A. Zeachandirin, P. Purcell and A. Cory, in *proceedings of the 16th Int. Symp. Packaging and Transportation of Radioactive Materials (PATRAM)*, London, U.K., 2010.

[6] D. Papaioannou, R. Nasyrow, V. V. Rondinella, W. Goll, H.-P. Winkler, R. Liedtke and D. Hoffmann, in *Proceedings of the KTG conference*, Dresden, Germany, 2009.

[7] "Final Report CRP SPAR III, IAEA-Tecdoc-1771," IAEA, 2015.

[8] R. Nasyrow, D. Papaioannou, V. V. Rondinella, E. Vlassopoulos, K. Linneman, V. Balheimer, J. Sterthaus, A. Rolle, F. Wille and S. Caruso, "Bending test device for mechanical integrity studies of spent nuclear fuel rods," in *Proc. 18th International Symposium on the Packaging and Transportation of Radioactive Materials (PATRAM)*, Kobe, Japan, 2016.

[9] K. Linnemann, V. Ballheimer, J. Sterthaus, A. Rolle, F. Wille, R. Nasyrow, D. Papaioannou, E. Vlassopoulos and V. V. Rondinella, in *Proc. 18th Int. Symp. Packaging and Transportation of Radioactive Materials (PATRAM)*, Kobe, Japan, 2016.

[10] V. V. Rondinella, R. Nasyrow, D. Papaioannou, E. Vlassopoulos, F. Cappia, O. Dieste-Blanco and T. Wiss, "Mechanical Integrity Studies on Spent Nuclear Fuel Rods," in *Proc. 16th International High-Level Radioactive Waste Management Conference (IHLRWM)*, Charlotte, U.S.A., 2017.

[11] E. Vlassopoulos, S. Caruso, R. Nasyrow, D. Papaioannou, R. Gretter and V. V. Rondinella, "Investigation of the properties and behaviour of spent nuclear fuel under conditions relevant for interim dry storage, handling and transportation: experimental setup optimisation and cold test campaign," Nagra Working Rep. NAB 16-067, Wettingen, Switzerland, 2017.

[12] E. Vlassopoulos, R. Nasyrow, D. Papaioannou, V. V. Rondinella, S. Caruso and A. Pautz, in *Proc. 16th International High-Level Radioactive Waste Management Conference (IHLRWM)*, Charlotte, U.S.A., 2017.

[13] E. Vlassopoulos, R. Nasyrow, D. Papaioannou, R. Gretter, L. Fongaro, J. Somers, V. V. Rondinella, S. Caruso, P. Grünberg, J. Helfenstein, P. Schwizer and A. Pautz, "Response of irradiated nuclear fuel rods to quasi-static and dynamic loads," *KERNTECHNIK,* vol. 83, p. 6, 2018.

[14] *ISO 7438:2016, Metallic materials - Bend test.*

[15] J. Arborelius, M. Dahlbäck, L. Hallstadius, P. Jourdain, T. Andersson, R. H. M. Lisdat and E. Toscano, "The Effect of Duplex Cladding Outer Component Tin Content," in *Zirconium in the Nuclear Industry: Fourteenth International Symposium, P. Rudling*, West Conshohocken, PA, USA, 2004.

[16] D. Papaioannou, E. Vlassopoulos, S. L. K. Caruso, R. Nasyrow, R. Gretter, L. Fongaro and V. Rondinella, “Experimental Studies on the Mechanical Stability of Spent Nuclear Fuel Rods,” in *GRS Workshop on Safety of Extended Dry Storage of Used Nuclear Fuel*, Garching, Germany, 2019.

[17] D. Papaioannou, E. Vlassopoulos, R. Nasyrow, R. Gretter, L. Fongaro, J. Somers, V. Rondinella and S. Caruso, “Mechanical Loading Tests on Irradiated LWR Fuel Rods,” in *IAEA International Conference on the Management of Spent Fuel, IAEA CN 272/51*, Vienna, Austria, 2019.

## List of abbreviations and definitions

| | |
|---|---|
| BU | Burn up |
| BWR | Bowling Water reactor |
| ECD | Equivalent Circle Diameter |
| FA | Fuel Assembly |
| HBS | High Burn-up Structure |
| IA | Image Analysis |
| JRC | Joint Research Centre |
| LWR | Light Water reactor |
| NPP | Nuclear Power Plant |
| PCI | Pellet Cladding Interaction |
| PIE | Post Irradiation Examinations |
| RCT | Ring Compression Test |
| SEM | Scanning electron Microscopy |
| SNF | Spent Nuclear Fuel |

## List of figures

## List of tables

## The European Commission's science and knowledge service

Joint Research Centre

### JRC Mission

As the science and knowledge service of the European Commission, the Joint Research Centre's mission is to support EU policies with independent evidence throughout the whole policy cycle.

**EU Science Hub**
ec.europa.eu/jrc

@EU_ScienceHub

EU Science Hub - Joint Research Centre

Joint Research Centre

EU Science Hub